Norouzian Baghani et al. Journal of Environmental Health Science & Engineering (2016) 14:11
DOI 10.1186/s40201-016-0252-0

Journal of Environmental Health Science and Engineering

RESEARCH ARTICLE Open Access

# One-Pot synthesis, characterization and adsorption studies of amine-functionalized magnetite nanoparticles for removal of Cr (VI) and Ni (II) ions from aqueous solution: kinetic, isotherm and thermodynamic studies

Abbas Norouzian Baghani[1,2], Amir Hossein Mahvi[2,3], Mitra Gholami[4,5*], Noushin Rastkari[6] and Mahdieh Delikhoon[7]

## Abstract

**Background:** Discharge of heavy metals such as hexavalent chromium (Cr (VI)) and nickel (Ni (II)) into aquatic ecosystems is a matter of concern in wastewater treatment due to their harmful effects on humans. In this paper, removal of Cr (VI) and Ni (II) ions from aqueous solution was investigated using an amino-functionalized magnetic Nano-adsorbent ($Fe_3O_4$-$NH_2$).

**Methods:** An amino-functionalized magnetic Nano-adsorbent ($Fe_3O_4$-$NH_2$) was synthesized by compositing $Fe_3O_4$ with 1, 6-hexanediamine for removal of Cr (VI) and Ni (II) ions from aqueous solution. The adsorbent was characterized by Scanning Electron Microscope (SEM), Transmission Electron Microscopy (TEM), powder X-Ray Diffraction (XRD), and Vibrating Sample Magnetometry (VSM). Also, the effects of various operational parameters were studied.

**Results:** According to our finding, $Fe_3O_4$-$NH_2$ could be simply separated from aqueous solution with an external magnetic field at 30 s. The experimental data for the adsorption of Cr (VI) and Ni (II) ions revealed that the process followed the Langmuir isotherm and the maximum adsorption capacity was 232.51 mg $g^{-1}$ for Cr (VI) at pH = 3 and 222.12 mg $g^{-1}$ and for Ni(II) at pH = 6 at 298 °K. Besides, the kinetic data indicated that the results fitted with the pseudo-second-order model ($R^2$: 0.9871 and 0.9947 % for Cr (VI) and Ni (II), respectively. The results of thermodynamic study indicated that: standard free energy changes ($\Delta G^{\ominus}$), standard enthalpy change ($\Delta H^{\ominus}$), and standard entropy change ($\Delta S^{\ominus}$) were respectively −3.28, 137.1, and 26.91 kJ $mol^{-1}$ for Cr (VI) and −6.8433, 116.7, and 31.02 kJ $mol^{-1}$ for Ni (II). The adsorption/desorption cycles of $Fe_3O_4$-$NH_2$ indicated that it could be used for five times.

**Conclusions:** The selected metals' sorption was achieved mainly via electrostatic attraction and coordination interactions. In fact, $Fe_3O_4$-$NH_2$ could be removed more than 96 % for both Cr (VI) and Ni (II) ions from aqueous solution and actual wastewater.

**Keywords:** $Fe_3O_4$-$NH_2$, Heavy metal ions, Amino-functionalized, 1, 6 hexanediamine, Thermodynamics, Adsorption/desorption

* Correspondence: gholamim@iums.ac.ir; gholamimitra32@gmail.com
[4]Research Center for Environmental Health Technology, Iran University of Medical Sciences, Tehran, Iran
[5]Environmental Health Department, School of Public Health, Iran University of Medical Sciences, Tehran, Iran
Full list of author information is available at the end of the article

## Background

Discharge of heavy metals into aquatic ecosystems is a matter of concern in wastewater treatment due to their harmful effects on humans even at low concentrations [1, 2]. Among heavy metals, Cr (VI) is among the toxic elements that may enter the environment due to effluent discharge by some industries, such as tanning, textile, wood preservations, paint, metal and mineral processing, pulp, and paper industries [3, 4]. Evidence has shown that these elements can be carcinogenic and mutagenic to living organisms [5]. Nickel is also another heavy metal used in different industries, such as porcelain enameling, electroplating, storage batteries, dying, steel manufacturing, and pigment industries. The acceptance tolerance of nickel has been reported to be 0.01 $mgL^{-1}$ and 2.0 $mgL^{-1}$ in drinking water and industrial wastewater, respectively [6]. Due to the problems remarked above, some effective wastewater treatment approaches have to be employed for Cr (VI) and Ni (II) removal. Up to now, many methods have been used in this regard, including chemical precipitation, ion exchange, membrane technologies, coagulation, electrocoagulation, reduction, bio sorption, filtration, adsorption, reverse osmosis, foam flotation, granular ferric hydroxide, electrolysis, and surface adsorption [7–11]. Most of these methods have economic and technical disadvantages and could not achieve the discharge standards. Yet, adsorption is an effective and flexible method, generating high-quality treated effluent [12]. Until now, many adsorbents have been grown, including maple sawdust, walnut, hazelnut, almond shell [2], carbon nanotubes [13], amino-functionalized polyacrylic acid (PAA) [14], and Lewatit FO36 Nano [15]. However, in many cases, these materials do not have the sufficient adsorption efficiency because of not having enough active surface sites. Furthermore, these materials have a lot of problems, including high cost, difficulty in separation, desorption, and regeneration of adsorbents, and secondary wastes. Therefore, new materials, such as various functional groups, including amide, amino groups, and carboxyl, are to develop new adsorbents that have high selectivity toward toxic metals [16–18]. In this respect, amino-groups have attracted more attention as chelation sites due to their large specific surface areas. Thus, amino-groups are capable of adsorbing a number of metal anions and cations from aqueous solution [19].

As described above, due to the high specific surface area created through grafting of appropriate organic amino-groups on inorganic magnetic $Fe_3O_4$ particles, with strong magnetic properties, low toxicity, and easy separation, it could be used as a sorbent for removing heavy metals [18, 20]. Another advantage is that it is useful for recovery or reuse of the magnetite nanoparticles modified with amino-groups [17, 21].

In this study, we prepared a novel amino-functionalized magnetic Nano-adsorbent ($Fe_3O_4$-$NH_2$) developed by grafting amino-groups onto the surfaces of $Fe_3O_4$ nanoparticles and used nanocompostie as the adsorbent for removal of Cr (VI) and Ni (II) from aqueous solution. The adsorbent was characterized by Transmission Electron Microscopy (TEM), powder X-Ray Diffraction (XRD), Vibrating Sample Magnetometry (VSM), Scanning Electron Microscope (SEM), and zeta-potential measurement. The effects of pH, initial concentrations of Cr (VI) and Ni (II), adsorption kinetics, thermodynamics, and adsorption isotherm were studied, as well.

## Methods

### Chemicals

Anhydrous sodium acetate, iron (III) chloridehexahydrat ($FeCl_3 \cdot 6H_2O$), potassium dichromate, ethanol, 1,6-hexanediamine, ethylene glycol, nickel (II) chloride hexahydrat ($NiCl_2.6H_2O$), sodium hydroxide, hydrogen chloride, which were of analytical grade, were purchased from Merck, Germany and were used without further purification. Potassium dichromate (99 %) and nickel (II) chloride hexahydrat (99 %) were used for preparation of Cr (VI) and Ni (II) solution. Additionally, doubly distilled deionized water was used throughout the work.

### Synthesis of amino-functionalized magnetic Nano-adsorbent ($Fe_3O_4$-$NH_2$) by one-pot synthesis

Amino-functionalized magnetic Nano-adsorbent ($Fe_3O_4$-$NH_2$) was prepared according to hydrothermal reduction method. In doing so, a solution of 1, 6-hexanediamine (13 g), anhydrous sodium acetate (4.0 g), and $FeCl_3 \cdot 6H_2O$ as a single Fe ion source (2.0 g) was added to ethylene glycol (80 mL). The above mixture was stirred at 50 °C under vigorous stirring for 30 min. Then, this solution was heated at 198 °C in a Teflonlined autoclave for 6 h. Thereafter, the mixture was cooled down to room temperature. The magnetite nanoparticles were collected with a magnet and were then washed with water and ethanol (3 times) to effectively remove the solvent and unbound 1, 6-hexanediamine. Finally, the amino-functionalized magnetic Nano-adsorbent ($Fe_3O_4$-$NH_2$) was dried in a vacuum oven at 50 °C before characterization and application [22]. The size and morphology of the $Fe_3O_4$-$NH_2$ were showed by SEM (Holland, company: Philips). Besides, the magnetic property (M–H loop) of the typical magnetic nanoparticles bound with 1, 6-hexadiamine at 25 °C was characterized by VSM (MDKFD, Iran). The crystal structure and phase purity of $Fe_3O_4$-$NH_2$ were also examined by XRD (Philips, Holland) using Cu Kα radiation (λ = 0.1541 nm) at $2^{\theta}$, 30 kV, and 30 mA. Finally, the TEM image of $Fe_3O_4$-$NH_2$ was examined using TEM, Model EM10C-100KV (Zeiss, Germany).

#### *Adsorption experiments*

The absorption experiments were conducted in 1000 ml Erlenmeyer flasks containing 50 ml Ni (II) and Cr (VI)

solutions at 5 to 100 mg $L^{-1}$ concentrations and 0.05 g of $Fe_3O_4$-$NH_2$. The mixtures were stirred (200 rpm) at room temperature from 10 to 90 min. After adsorption, $Fe_3O_4$-$NH_2$ with adsorbed Cr (VI) and Ni (II) was separated from the solution under the external magnetic field. The concentrations of Cr (VI) and Ni (II) ions in the solutions were measured by an Inductive Coupled Plasma (ICP-OES, Spectro arcos, Germany (Company: SPECTRO)).

In order to determine the effects of various factors, the experiments were performed at different $Fe_3O_4$-$NH_2$ doses (0.1 to 0.3 g/L), initial concentrations of Cr (VI) and Ni (II) (5 to 100 mg/L), and temperatures (298.15 to 338.15 °K). Besides, each experiment was carried out in duplicate. The removal of Cr (VI) and Ni (II) by $Fe_3O_4$-$NH_2$ and removal efficiency have been figured by equations in Table 1 [18].

## Results and Discussion

### Characterization of $Fe_3O_4$-$NH_2$

The SEM, VSM, XRD, and TEM of $Fe_3O_4$-$NH_2$ were recorded. The SEM of $Fe_3O_4$-$NH_2$ image has been shown in Fig. 1. Based on the results, the SEM image indicated that the size of $Fe_3O_4$-$NH_2$ was much smaller than that of naked particles, confirming the coating of 1, 6 hexanediamine [18].

The magnetic hysteresis loops measured at room temperature has been illustrated in Fig. 2. The M–H curves showed that $Fe_3O_4$ and $Fe_3O_4$-$NH_2$ were essentially super-paramagnetic. $Fe_3O_4$-$NH_2$ and $Fe_3O_4$ have a magnetization saturation value of 73.25 and 91.57 emu $g^{-1}$, respectively. According to Fig. 3, the magnetic $Fe_3O_4$-$NH_2$ was dispersed in water. In addition, it could be collected by external magnetic field and be re-dispersed through slight shaking, making the solid and liquid phases separate easily.

The XRD patterns of $Fe_3O_4$-$NH_2$ have been shown in Fig. 4. In this study, the crystal structure and phase purity of $Fe_3O_4$-$NH_2$ were examined by XRD using a Cu Kd radiation (λ = 0.1541 nm) at $2^{\theta}$ of 30.1°, 35.5°, 43.1°, 53.4°, 57.0°, and 62.6° corresponding to their indices; i.e., 220, 311, 400, 422, 511, and 440, at 30 kV and 30 mA. The particle size was obtained via XRD analysis through Debye-Sherrer's formula [23]: D = K λ/β COS θ.

Where λ is the wavelength of the X-rays, θ is the diffraction angle, and β is the corrected full width. The result of size distribution demonstrated that the size of the prepared $Fe_3O_4$-$NH_2$ was under 90 nm. Additionally, the sharp and strong peaks of the products revealed its appropriate crystallinity. Moreover, the six characteristic peaks of $Fe_3O_4$ showed that amino-groups did not cause any measureable alter in the phase property of $Fe_3O_4$ cores. Therefore, the amino-groups were fixed on the surface of $Fe_3O_4$ cores, making a core-shell structure. In other words, binding and amino-functionalization ($NH_2$) occurred only on the surface of $Fe_3O_4$ cores to form a core−shell structure [22].

The TEM image of $Fe_3O_4$-$NH_2$ has been shown in Fig. 5. Accordingly, $Fe_3O_4$-$NH_2$ particles were multidispersed with an average diameter of around 25 nm. It has been reported that magnetic particles of less than 30 nm would show paramagnetism [24].

### The effect of initial concentration and pH on the adsorption properties and zeta potential analyses

The effect of initial concentration on the adsorption properties was intensively studied for $Fe_3O_4$-$NH_2$ by varying $C_0$ of Cr (VI) and Ni (II) ions at 5, 25, 50, and 100 mg $L^{-1}$. The results have been presented in Figs. 6 and 7. Under corresponding pH values from 2.0 to 9.0, the adsorption efficiency of Cr (VI) and Ni (II) respectively decreased and increased with increase in the initial Cr (VI) and Ni (II) concentrations. Accordingly, the percentage of uptake of Cr (VI) and Ni (II) ions at the $Fe_3O_4$-$NH_2$ concentration of 5 mg $L^{-1}$ decreased from 98.02 to 36.85 % for Cr (VI) and increased from 46.21 to 93.03 % for Ni (II) with increasing the pH from 2.0 to 9.0. This can be justified by the fact that for a fixed adsorbent dosage, the total available adsorption sites would be relatively settled. Thus, increasing the initial Cr (VI) and Ni (II) concentrations led to a decrease in the adsorption percentage of the adsorbate [25].

**Table 1** The kinetic, isotherm, and thermodynamic equations used for adsorption of Cr (VI) and Ni (II) onto $Fe_3O_4$-$NH_2$

| Kinetic models | Isotherm equations | Thermodynamic equations | Removal efficiency and equilibrium adsorption capacity | Ref. |
|---|---|---|---|---|
| Pseudo-first-order $\ln(q_e - q_t) = lnq_e - k_1 t$ | Freundlich isotherm $lnq_e = lnK_F + \frac{1}{n}\ln Ce$ | Van' t Hoff $\Delta G^{\theta} = -RTlnK$ | equilibrium adsorption capacity $q_e = \frac{(C0-Ce)V}{m}$ | [31–38] |
| Pseudo-second-order $\frac{t}{qt} = \frac{1}{K_2 q_{e.c}^2} + \frac{t}{q_{e.c}}$ | Langmuir adsorption model $\frac{C_e}{q_e} = \frac{1}{K_l q_m} + \frac{C_e}{q_m}$ | Free energy of adsorption $\mathrm{Ln}K = -\frac{\Delta H\theta}{RT} + \frac{\Delta S\theta}{R}$ | Removal efficiency $(\%) = \frac{(C_i - C_o)}{C_i} \times 100$ | [27, 31, 33–37, 39] |
| | Separation factor ($R_L$) $R_L = 1/(1 + K_L C_o)$ | | | [18, 25, 26] |

qe (mg/g), $K_1$ (1/min), $K_2$ (g/mgmin), qm (mg/g), $K_F$ [(mg $g^{-1}$) ($mgL^{-1}$) n], Kp (mg/g $min^{-0.5}$), $C_0$ (mg/L), $\Delta H^{\theta}$ (kJ/mol), $\Delta S^{\theta}$ (J/mol.K), T (K), R (8.314 J/mol.K),V (mL), m (mg)

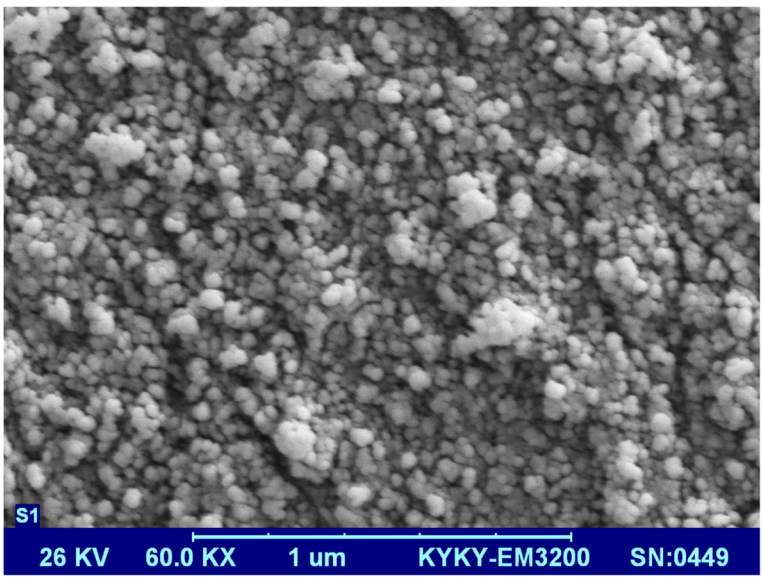


**Fig. 1** SEM image of $Fe_3O_4$ -$NH_2$

To assess the effect of pH, the study was conducted from pH 2 to 9 for both Cr (VI) and Ni (II) ions. The maximum sorption was perceived at pH = 6 for Ni (II), but at pH = 3 for Cr (VI). The adsorption of Cr (VI) at lower pH levels was also observed in other magnetic materials, such as the mesoporous magnetic ɤ-$Fe_2O_3$ [26]. pH value affected the adsorption efficiency due to its influence on the amino-groups modified on the surface of $Fe_3O_4$-$NH_2$. The plot of pH initial vs. pH final depicted that the pHzpc was 5.8 for $Fe_3O_4$–$NH_2$. Hence, at pH >5.8, the surface charge of $Fe_3O_4$-$NH_2$ was negative and the electrostatic interactions between the metal ions and the adsorbent enhanced. Considering Ni (II), the interaction between the adsorbents and the Ni (II) ions might be defined by Equations 1–5 [14, 27].

$$R-NH_2+H^+\leftrightarrow R-NH_3^+(\text{amino protonate}) \quad (1)$$

$$R-NH_2+Ni^{2+}\leftrightarrow R-NH_2Ni^{2+} \quad (2)$$

$$R-NH_2+OH^-\leftrightarrow R-NH_2OH^- \quad (3)$$

$$R-NH_2OH^-+Ni^{2+}\leftrightarrow R-NH_2OH^-\ldots Ni^{2+} \quad (4)$$

$$\text{Or } R-NH_2OH^-+NiOH^+\leftrightarrow R-NH_2OH^-\ldots NiOH^+ \quad (5)$$

The protonation/deprotonation reactions of the $Fe_3O_4$-$NH_2$ amino-groups in the solution have been presented in Equation 1. Based on Equation 2, the ability of $NH_2$ to be protonated was weakened at higher pH levels, resulting in more –$NH_2$ on the surface of the adsorbent

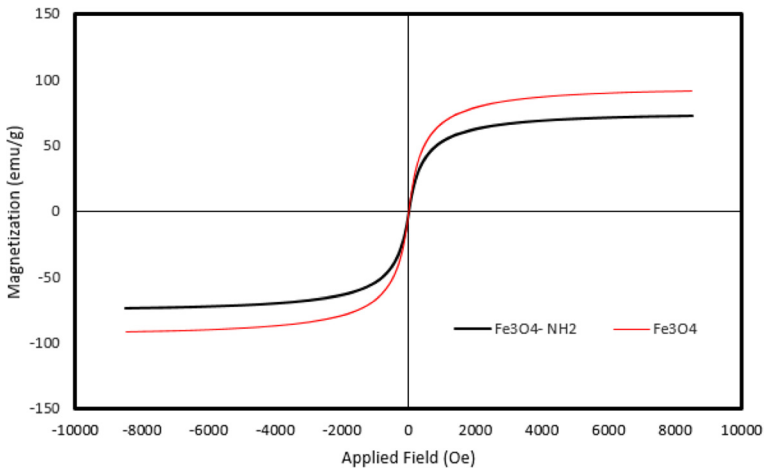


**Fig. 2** VSM magnetization curves of $Fe_3O_4$-$NH_2$ and $Fe_3O_4$


**Fig. 3** Demonstration of magnetic separation at 30 s

to coordinate with Ni (II). At higher pH levels, $OH^-$ in the solution is competitively adsorbed by amino-groups ($-NH_2$), and the electrostatic adsorption is prevailed gradually compared to coordination. Considering Cr (VI), a large number of $H^+$ exists under acidic conditions (pH levels: 2–3.5), causing amino-groups ($-NH_2$) to be protonated to $NH^{3+}$ more easily and electrostatic attraction to occur between these two oppositely charged ions (Equation (6)) [14, 27].

$$R - NH^{3+} + HCro_4^- \rightarrow R - NH^{3+} \ldots\ldots HCro_4^- \quad (6)$$

### Kinetic, equilibrium, and thermodynamic studies

Adsorption isotherms of $Fe_3O_4$-$NH_2$ were gained at pH = 3 for Cr (VI) and pH = 6 for Ni (II) with the initial concentrations of 5 to 100 mg $L^{-1}$. The relevant equations for kinetic, equilibrium, and thermodynamic studies have been shown in Table 1 [18]. Besides, the Langmuir and

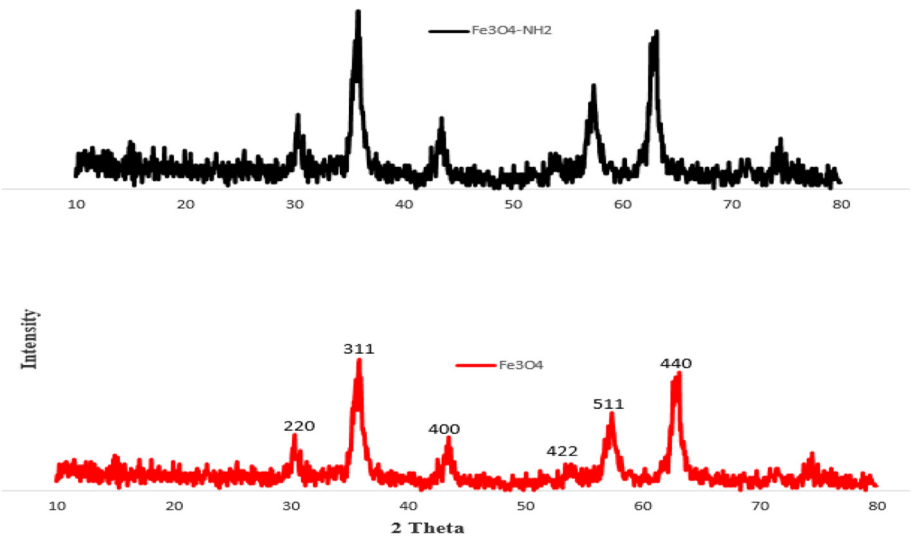


**Fig. 4** XRD for $Fe_3O_4$-$NH_2$ and $Fe_3O_4$

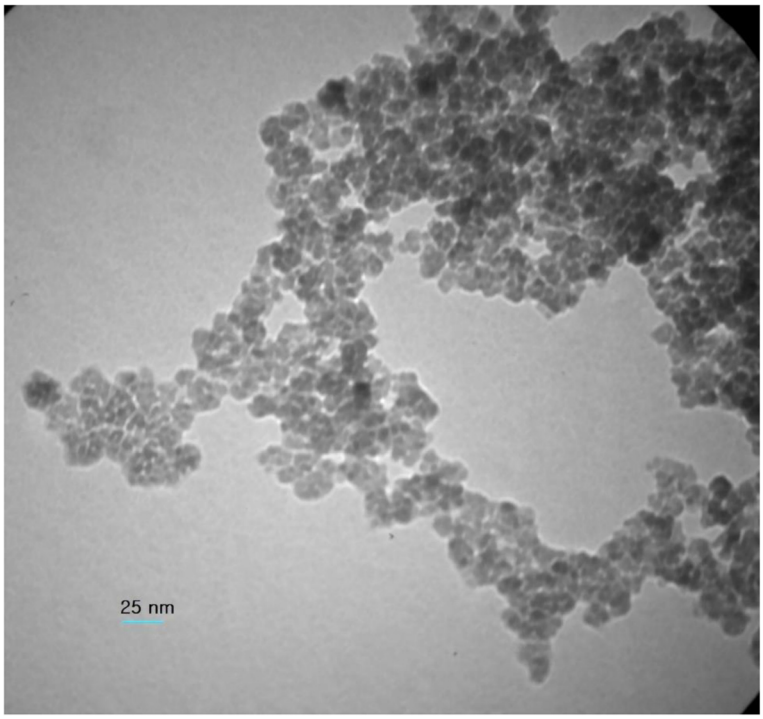


**Fig. 5** TEM image of $Fe_3O_4$-$NH_2$

Freundlich parameters, correlation coefficients ($R^2$), and separation factor ($R_L$) for the adsorption of Cr (VI) and Ni (II) on $Fe_3O_4$-$NH_2$ have been summarized in Table 2. The essential characteristics of the Langmuir isotherm can be expressed in terms of a dimensionless separation factor ($R_L$). The plot of $C_e$ vs. ($C_e/q_e$) for $Fe_3O_4$-$NH_2$ gave a straight line with correlation coefficients of 0.998 and 0.994 for Cr (VI) and Ni (II), respectively. The $q_{max}$ and $K_L$ were derived from the slope and intercept of the line, respectively. The adsorption capacities ($q_m$, mg/g) using the Langmuir isotherm equation were as follows: $q_m$ Ni (II) (232.15) > $q_m$ Cr (VI) (222.12). Considering the larger adsorption capacity of $Fe_3O_4$-$NH_2$ attributed to the amino-groups modified on the surface of $Fe_3O_4$-$NH_2$, the amino-groups played a very important role in the adsorption process of Cr (VI) and Ni (II) in aqueous solution. This implies that increasing the percentage of nitrogen in the $Fe_3O_4$-$NH_2$ could increase the value of $q_m$. The calculated $R_L$ values for adsorption of Cr (VI) and Ni (II) were also 0.03–0.39 and 0.02–0.34, respectively, which fall between 0 and 1. Thus, the adsorption of Cr (VI) and Ni (II) onto $NH_2$- $Fe_3O_4$ was favorable. However, the correlation coefficients ($R^2 > 0.99$) and $R_L$ ($0 < R_L < 1$) proved that the Langmuir isotherm fitted better for adsorption of Cr (VI) and Ni (II) on $NH_2$- $Fe_3O_4$. On the other hand, the value of 1/n shows whether the adsorption is suitable for the

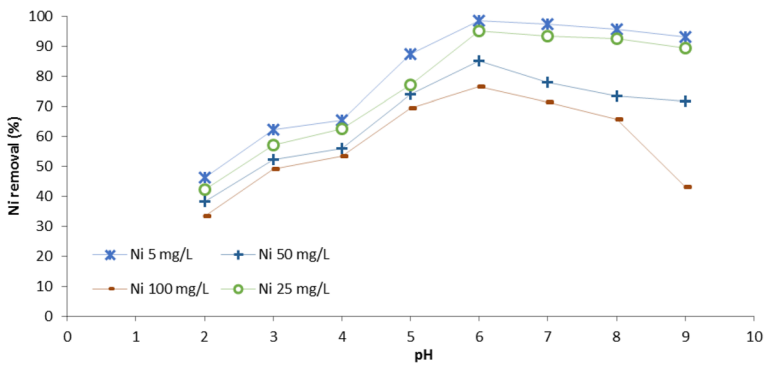


**Fig. 6** The effect of pH on the adsorption of Ni (II) onto $Fe_3O_4$-$NH_2$ at different initial concentrations

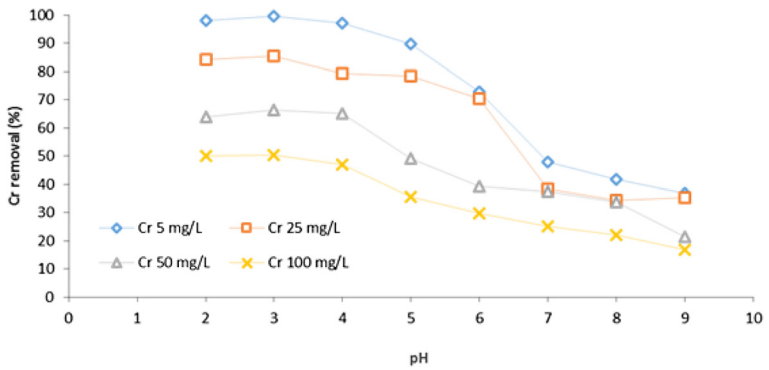


**Fig. 7** The effect of pH on the adsorption of Cr (VI) onto $Fe_3O_4$-$NH_2$ at different initial concentrations

Freundlich isotherm [18]. The value of 1/n reported in Table 2 was less than 1; hence, adsorption by the Freundlich model was unfavorable. Kinetics of the adsorption process is essential for aqueous solution since it gives essential information on the rate of adsorbate uptake on the adsorbent and controls the equilibrium time. The results presented in Table 2 indicated that the adsorption capacity of $Fe_3O_4$-$NH_2$ for Cr (VI) and Ni (II) was high ($q_m$ for Ni (II) = 232.51 mg/$g^{-1}$ at pH = 6 and $q_m$ for Cr (VI) = 222.12 mg/$g^{-1}$ at pH = 3) compared to other adsorbents. Afkhami et al. also reported that the adsorption capacity of DNPH-γ-$Al_2O_3$ for Ni (II) was 18.18 (mg $g^{-1}$) at pH = 5 and that the process followed the Langmuir isotherm [26]. In another study, the experimental data for the adsorption of Ni (II) on $Fe_3O_4$-GS revealed that the process followed the Langmuir isotherm and that the maximum adsorption capacity was 158.5 mg $g^{-1}$ at pH = 6 [28]. The parameters of the pseudo-first-order and pseudo-second-order sorption kinetic models have been presented in Table 3. In order to evaluate the applicability of these kinetic models to fit the experimental data, $K_1$ and $K_2$ constants were determined experimentally from the slope and intercept of straight-line plots. The value of qe.c earned from the pseudo-second-order model was 28.25 mg $g^{-1}$ for Cr (VI) and 25.97 mg $g^{-1}$ for Ni (II) ions, which perfectly corresponded to the experimental values of qe (24.25 and 25.12 mg $g^{-1}$) for Cr (VI) and Ni (II) ions. Overall, the pseudo-second-order model ($R^2$: 0.9871 and 0.9947 % for Cr (VI) and Ni (II), respectively) was more efficient compared to the pseudo-first-order model ($R^2$: 0.8422 and 0.8862 % for Cr (VI) and Ni (II), respectively). Because all the correlation coefficients were higher than 0.98 %, Cr (VI) and Ni (II) adsorption onto $Fe_3O_4$-$NH_2$ might take place through a chemical process involving valence forces through sharing or exchange of electrons [25]. In another kinetic study using $Fe_3O_4$-adsorbent, $R^2$ value of Ni (II) was 0.998 at the optimum pH of 5.5. Therefore, the results showed that Ni (II) adsorption on $Fe_3O_4$ could be followed by the Freundlich model [29]. In order to measure the thermodynamic parameters for Cr (VI) and Ni (II) adsorption on $Fe_3O_4$-$NH_2$, the adsorption studies were accomplished at 298.15 to 313.15 °K. The negative values of $\Delta G^\theta$ at different temperatures, positive value of $\Delta S^\theta$, and positive value of $\Delta H^\theta$ during the adsorption of Cr (VI) and Ni (II) on $Fe_3O_4$-$NH_2$ indicated that the adsorption was spontaneous, increased randomness at the solid-solution interface, and was endothermic in nature [18]. In addition, the slope and intercept of the plot of lnK vs. 1/T indicated the $\Delta H^\theta$ and $\Delta S^\theta$ values [18]. The values of standard enthalpy change ($\Delta H^\theta$) and standard entropy change ($\Delta S^\theta$), which were related to distribution coefficient ($K_D$), were calculated and presented in Table 2. Using the $\Delta H^\theta$ and $\Delta S^\theta$ values, standard free energy changes ($\Delta G^\theta$) for $Fe_3O_4$-$NH_2$ were estimated. The results indicated that adsorption of Cr (VI) and Ni (II) on $Fe_3O_4$-$NH_2$ could be followed spontaneously, was endothermic, and was entropy favored in nature. The positive value of $\Delta S^\theta$ proved increase in the randomness at the solid-solution interface during the adsorption of Cr (VI) and Ni (II) on $Fe_3O_4$-$NH_2$. This indicated that the amino-functionalized magnetic Nano-adsorbent ($Fe_3O_4$-$NH_2$) could be regarded as an efficient and low cost adsorbent. The results of thermodynamic study in our research indicated that ΔG, ΔH, and ΔS were respectively −3.28, 137.1, and 26.91 kJ $mol^{-1}$ for Cr (VI) and −6.8433, 116.7, and 31.02 kJ $mol^{-1}$ for Ni (II). Shen et al. conducted a similar study using adsorbent DETA-NMPs and disclosed that ΔG, ΔH, and ΔS were −13.7, 8.41, and 72.83 kJ $mol^{-1}$, respectively for Cr (VI) [25]. Hence, the results indicated that adsorption of Ni (II) on DETA-NMPs could be followed spontaneously, was endothermic, and was entropy favored in nature [25]. One other study also reported that ΔG, ΔH, and ΔS were −1.599, 8.438, and 83.1, respectively for Ni (II) adsorption on Nano-HAP [30].

Overall, simple preparation, fast separation, and high adsorption capacity of $Fe_3O_4$-$NH_2$ make it a potential

**Table 2** The kinetic and thermodynamic and isotherm constants for the adsorption of Cr (VI) and Ni (II) by $Fe_3O_4$ $NH_2$ and other adsorbents

| Tem. | Adsorbent | pH | | Pseudo-second-order | | | Thermodynamic parameters | | | | Ref. |
|---|---|---|---|---|---|---|---|---|---|---|---|
| (k) | | Cr (VI) | Ni (II) | $K_2$ (g/mg$^{-1}$) (min)$^{-1}$ | $q_{e,cal}$ (mg/g$^{-1}$) | $R^2$ | $\Delta G^e$ (kJ mol$^{-1}$) | $\Delta H^e$ (kJmol$^{-1}$) | $\Delta S^e$ (J (mol K)$^{-1}$) | | |
| 308 | EDA-NMPs | 2.5 | - | 0.7862 | - | 1 | −1.61 | 10.59 | 37.50 | | [25] |
| 308 | DETA-NMPs | 2.5 | - | 0.3668 | - | 1 | −1.76 | 9.67 | 34.64 | | [25] |
| 308 | TETA- NMPs | 2.5 | - | 0.3219 | - | 1 | −2.15 | 23.15 | 76.82 | | [25] |
| 308 | TEPA- NMPs | 2.5 | - | 0.1042 | - | 1 | −2.36 | 10.46 | 38.04 | | [25] |
| 303 | Activated Alumina | 3 | - | - | 0.0757 | 0.999 | 9.78 | - | - | | [40] |
| 298 | LewaitMP 610 | 5 | - | - | - | - | −10.40 | −2.51 | 35.49 | | [5] |
| 298 | $Fe_3O_4$ | - | 6 | 0.004 | | 0.998 | - | - | - | | [41] |
| 298 | ZnO | - | 6 | 0.002 | | 0.998 | - | - | - | | [41] |
| 298 | CuO | - | 6 | 0.019 | | 0.995 | - | - | - | | [41] |
| 303 | Bagass Fly ash | 5 | - | - | - | - | −1.46 | 14.24 | 49 | | [42] |
| 293 | Nano-HAP | - | 6.6 | - | - | - | −1.599 | 8.438 | 83.1 | | [30] |
| 298 | Superparamagnetic Iron Oxide | - | 5.5 | - | - | - | 27.9 | 7.8 | 110 | | [29] |
| 293 | $Fe_3O_4$-GS | 2 | - | 0.055 | 17.29 | 0.999 | −4.182 | 76.63 | 18.28 | | [28] |
| 293 | $Fe_3O_4$-GS | - | 6 | 0.0203 | 22.07 | 0.998 | −3.456 | 31.86 | 5.965 | | [28] |
| 323 | $Fe_3O_4$-TW | - | 6 | - | - | - | 10.02 | 33.41 | 0.5799 | | [6] |
| 298 | Waste tea | - | 4 | - | - | - | −3.82 | 17.07 | 20.92 | | [43] |
| 313 | DETA-NMPs | - | 6 | 1.03 | 9 | 0.999 | −13.7 | 8.41 | 72.83 | | [25] |
| 298 | $Fe_3O_4$-$NH_2$ | 3 | - | 0.002 | 28.25 | 0.987 | −3.2891 | 137.1 | $\Delta S^e$ | $R^2$ | This study |
| | | | | | | | | | 26.91 | 0.975 | |
| 298 | $Fe_3O_4$-$NH_2$ | - | 6 | 0.008 | 25.97 | 0.994 | −6.8433 | 116.7 | 31.02 | 0.960 | This study |
| 303 | $Fe_3O_4$-$NH_2$ | Cr (VI) | Ni (II) | - | - | - | $\Delta G^e$Cr (VI) | | $\Delta G^e$Ni (II) | | This study |
| | | 3 | 6 | | | | −5.5038 | | −8.424 | | |
| 308 | $Fe_3O_4$-$NH_2$ | 3 | 6 | - | - | - | −9.7477 | | −10.045 | | This study |
| 313 | $Fe_3O_4$-$NH_2$ | 3 | 6 | - | - | - | −13.234 | | −12.934 | | This study |
| If: RL > 1, the adsorption is unfavorable. RL = 1, the adsorption is linear. 0 < RL < 1, the adsorption is favorable. RL = 0, the adsorption is irreversible. | | | | | | | | | | | [17, 44, 45] |
| If: 1/n < 1, the adsorption is unfavorable. If: 0.1 < 1/n < 1, the adsorption is favorable. | | | | | | | | | | | [46] |
| Tem. | Adsorbent | pH | | Freundlich constants | | | Langmuir constants | | | | Ref. |
| (k) | | Cr (VI) | Ni (II) | $K_F$ (Lg$^{-1}$) | n | $R^2$ | $q_{max}$ (mg g$^{-1}$) | $K_L$ (Lmg$^{-1}$) | | $R^2$ | |
| 308 | EDA-NMPs | 2.5 | - | - | - | - | 136.98 | 0.1648 | | 0.999 | [25] |
| 308 | DETA-NMPs | 2.5 | - | - | - | - | 149.25 | 0.4467 | | 0.999 | [25] |
| 308 | TETA- NMPs | 2.5 | - | - | - | - | 204.08 | 0.075 | | 0.998 | [25] |

**Table 2** The kinetic and thermodynamic and isotherm constants for the adsorption of Cr (VI) and Ni (II) by $Fe_3O_4$ $NH_2$ and other adsorbents *(Continued)*

| | | | | | | | | | | | |
|---|---|---|---|---|---|---|---|---|---|---|---|
| 308 | TEPA- NMPs | 2.5 | - | - | - | - | 370.37 | 0.1233 | | 0.999 | [25] |
| 298 | Walanut | 3.5 | - | 0.244 | 3.36 | 0.989 | 8.01 | 2.98 | | 0.964 | [2] |
| 298 | Hazelnut | 3.5 | - | 0.386 | 2.38 | 0.992 | 8.28 | 4.42 | | 0.976 | [2] |
| 298 | Almand Shells | 3 | - | 0.153 | 2.68 | 0.984 | 3.40 | 0.580 | | 0.972 | [2] |
| 303 | Activated Alumina | 3 | - | 2.84 | 1.80 | 09880 | 25.57 | 0.467 | | 0.991 | [40] |
| 298 | Mag | 2.5 | - | 4.90 | 2.94 | 0.729 | 20.16 | 0.262 | | 0.998 | [47] |
| 298 | MagDt-H | 2.5 | - | 1.62 | 2.63 | 0.984 | 13.88 | 0.030 | | 0.965 | [47] |
| 298 | Lewait MP 610 | 5 | - | - | - | - | .41 | - | | 0.99 | [5] |
| 298 | PAC | - | 8 | 0.02 | 2.85 | 0.708 | 31.08 | 0.27 | | 0.98 | [48] |
| 298 | Bagass | - | 8 | 1.4E-03 | 0.868 | 0.868 | 0.03 | 0.95 | | 0.97 | [48] |
| 298 | Fly ash | - | 8 | 2.03E-04 | 0.696 | 0.811 | 0.001 | 0.95 | | 0.98 | [48] |
| 298 | $Fe_3O_4$ | - | 6 | 1.550 | 0.996 | - | - | - | | - | [41] |
| 298 | ZnO | - | 6 | 0.319 | 0.991 | - | - | - | | - | [41] |
| 298 | CuO | - | 6 | 0.162 | 0.992 | - | - | - | | - | [41] |
| 303 | Bagass Fly ash | 5 | - | 1.86 | 12.05 | - | 4.35 | 0.014 | | 0.987 | [42] |
| 298 | $NH_2$_MCM-41 | 5 | - | 2.759 | 2.2 | 0.900 | 12.36 | 0.2245 | | 0.956 | [49] |
| 293 | Nano-HAP | - | 6.6 | 8.87 | 2.74 | 0.934 | 46.17 | 0.07 | | 0.995 | [30] |
| 298 | DNPH-γ-$Al_2O_3$ | - | 5 | 1.95 | 2.037 | 0.926 | 18.18 | 1.426 | | 0.985 | [26] |
| 293 | $Fe_3O_4$-GS | 2 | - | 30.58 | 3.01 | 0.997 | 39.92 | 4.08 | | 0.959 | [28] |
| 293 | $Fe_3O_4$-GS | - | 6 | 3.801 | 2.56 | 0.993 | 158.5 | 0.2830 | | 0.966 | [28] |
| 323 | $Fe_3O_4$-TW | - | 6 | 4.85 | 1.78 | 0.975 | 38.30 | 0.085 | | 0.996 | [6] |
| 298 | Superparamagnetic Iron Oxide | - | 5.5 | 0.113 | 0.213 | 0.986 | 0.189 mmol/g | 1.39 L/mmol | | 0.999 | [29] |
| 298 | Waste tea | - | 4 | 0.258 | 0.93 | 0.922 | 15.26 | 0.088 | | 0.996 | [43] |
| 333 | $Fe_3O_4$ -CNTs | - | 2 | 7.23 | 3.05 | 0.981 | 65.96 | 0.42 | | 0.997 | [44] |
| 313 | DETA-NMPs | - | 6 | 1.304 | 2.54 | 09026 | 43.24 | 0.288 | | 0.999 | [25] |
| 298 | $Fe_3O_4$-$NH_2$ | 3 | - | 1.13 | 2.05 | 0.940 | 222.12 | KL | RL | 0.995 | This study |
| | | | | | | | | 0.314 | 0.03-0.39 | | |
| 298 | $Fe_3O_4$-$NH_2$ | - | 6 | 1.44 | 1.83 | 0.979 | 232.51 | 0.383 | 0.02-0.34 | 0.988 | This study |
| If: RL > 1, the adsorption is unfavorable. RL = 1, the adsorption is linear. 0 < RL < 1, the adsorption is favorable. RL = 0, the adsorption is irreversible. | | | | | | | | | | | [17, 44, 45] |
| If: 1/n < 1, the adsorption is unfavorable. If: 0.1 < 1/n < 1, the adsorption is favorable. | | | | | | | | | | | [46] |

**Table 3** Kinetic adsorption parameters obtained using Pseudo-first-order and Pseudo-second-order models

| $Fe_3O_4$-$NH_2$ | Pseudo-first-order | | | | Pseudo-second-order | | |
|---|---|---|---|---|---|---|---|
| Metals | $K_1$ ($min^{-1}$) | $q_{e,exp}$ ($mg/g^{-1}$) | $q_{e,cal}$ ($mg/g^{-1}$) | $R^2$ | $K_2$ ($g/mg^{-1}$) $(min)^{-1}$ | $q_{e,cal}$ ($mg/g^{-1}$) | $R^2$ |
| Cr (VI) | 0.06 | 24.25 | 06.41 | 0.8422 | 0.002 | 28.25 | 0.9871 |
| Ni (II) | 0.03 | 25.12 | 14.64 | 0.8862 | 0.008 | 25.97 | 0.9947 |

applicant for Cr (VI) and Ni (II) removal. Considering the larger adsorption capacity of $Fe_3O_4$-$NH_2$ attributed to the amino-groups modified on the surface of $Fe_3O_4$-$NH_2$, the amino-groups played a very important role in the adsorption process of Cr (VI) and Ni (II) in aqueous solution. This indicated that the increase of nitrogen percentage in $Fe_3O_4$-$NH_2$ could result in an increase in the value of $q_m$. Similar results were also obtained by Shen et al. [27] and Zhao et al. [25].

### Desorption and reusability of $Fe_3O_4$-$NH_2$

For practical application of a cost-effective adsorbent for Cr (VI) and Ni (II) removal, desorption of metal ions from adsorbent and regeneration of $Fe_3O_4$-$NH_2$ is of particular importance. Since the adsorption of Cr (VI) and Ni (II) onto $Fe_3O_4$-$NH_2$ highly depends on the solution pH, desorption of the two heavy metals can be achieved by adjusting the pH. In the present study, the adsorption reversibility of Cr (VI)-laden $Fe_3O_4$-$NH_2$ and Ni (II)-laden $Fe_3O_4$-$NH_2$ was examined using NaOH (0.01, 0.05, 0.1, 0.2, and 0.3 mol $L^{-1}$) and $HNO_3$ (0.001, 0.005, 0.01, 0.05, and 0.1 mol $L^{-1}$). For desorption studies, the metal-adsorbed modified $Fe_3O_4$ nanoparticles were first washed by ultrapure water for three times to remove the unadsorbed metals loosely appended to the adsorbent. When the concentration of NaOH and $HNO_3$ was increased, the removal efficiency of desorption increased, as well. The best result was achieved with 2 min sonication in the presence of 0.2 mol $L^{-1}$ NaOH and 0.05 mol $L^{-1}$ $HNO_3$. Finally, the $Fe_3O_4$-$NH_2$ was dried in an oven (at 50 °C) during regeneration. In our study, each sorption/desorption process experienced a base and a heat treatment. The adsorption/desorption cycle results showed that the $Fe_3O_4$-$NH_2$ could be reused for 5 times. Besides, the results presented in Fig. 8 indicated that at the end of the fifth cycle, the $Fe_3O_4$-$NH_2$ maintained more than 76.19 % of its original Cr (VI) adsorption capacity and 77.13 % of its original Ni (II) adsorption capacity. Therefore, the great reusability $Fe_3O_4$-$NH_2$ demonstrated its good potential for practical application.

### The effect of real water matrix

In this study, 1.0 and 5 mg $L^{-1}$ Cr (VI) and Ni (II) were spiked with tap water and industrial wastewater for evaluating the practical application of $Fe_3O_4$-$NH_2$. The initial concentration, pH, and removal efficiencies of Cr (VI) and Ni (II) after treatment with $Fe_3O_4$-$NH_2$ have been presented in Table 4. According to the results, the removal efficiency of Cr (VI) at the concentration of 1.0 mg $L^{-1}$ was 97.94 and 98.56 % for tap water and industrial wastewater, respectively. These measures were respectively obtained as 96.12 and 97.24 % for Ni (II) at the concentration of 1.0 mg $L^{-1}$. This implies the excellent potential of $Fe_3O_4$-$NH_2$ in water and wastewater treatment.

## Conclusion

In this study, $Fe_3O_4$-$NH_2$ was prepared using a simple, cost-effective, and environmentally friendly method for the removal of Cr (VI) and Ni (II) ions from aqueous solution and was characterized by SEM, TEM, XRD, and VSM. The effects of controlling parameters, such as

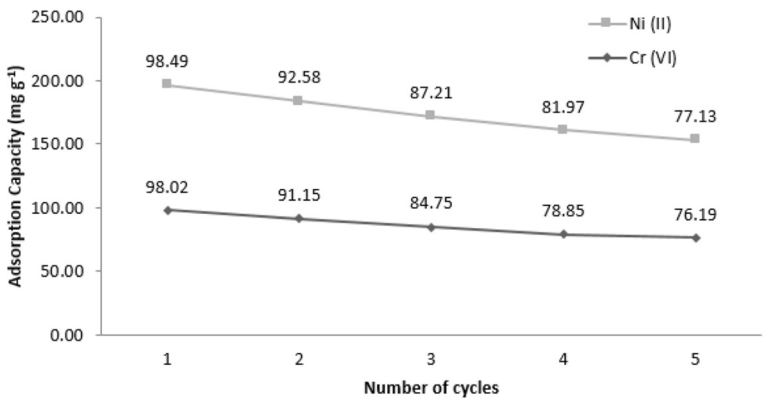


**Fig. 8** Adsorption and desorption efficiency of Cr (VI) and Ni (II) by $Fe_3O_4$-$NH_2$ in adsorption—desorption cycle

**Table 4** The adsorption efficiencies of Cr (VI) and Ni (II) by $Fe_3O_4$-$NH_2$ from tap water and industrial wastewater

| Matrix | $pH_{Cr(VI)}$ and $pH_{Ni(II)}$ | $Cr(VI)_{initial}$ and $Ni(II)_{initial}$ (mg $L^{-1}$) | $Cr(VI)_{removal}$ (%) | $Ni(II)_{removal}$ (%) |
|---|---|---|---|---|
| Tap water | 6.6 | 1 | 97.94 | 98.56 |
| Tap water | 6.6 | 5 | 96.85 | 97.61 |
| Industrial wastewater | 6.2 | 1 | 96.12 | 97.74 |
| Industrial wastewater | 6.2 | 5 | 95.25 | 96.42 |

contact time, temperature, pH, $Fe_3O_4$-$NH_2$ dose, and initial concentration of both heavy metals, were studied, as well. Based on the results, the Langmuir model fitted the isotherm data for both heavy metals and the maximum sorption capacity was 232.51 mg $g^{-1}$ at pH = 3 for Cr (VI) and 222.12 mg $g^{-1}$ at pH = 6 for Ni (II). Moreover, the adsorption kinetic data for Cr (VI) and Ni (II) were based on the assumption of a pseudo-second-order model and thermodynamic parameters showed that the adsorption process was endothermic, spontaneous, and entropy favored in nature. In addition, this nano-adsorbent was able to remove over 96 % of both heavy metals from tap water and industrial wastewater. The $Fe_3O_4$-$NH_2$ could be regenerated with acid after adsorption and the adsorption capabilities only decreased with 6-7 % for both metal ions after five cycles. Overall, this study indicated that an amino-functionalized magnetic nano-adsorbent was promising for removal of Cr (VI) and Ni (II) ions in field application.

## Highlights

A sensitive method was developed for removal of Cr (VI) and Ni (II) from aqueous solution.

In-lab synthesized magnetic nanoadsorbent was developed by grafting amino-groups onto the surfaces of $Fe_3O_4$ nanoparticles.

The adsorbent was characterized by Transmission Electron Microscopy (TEM), powder X-Ray Diffraction (XRD), Vibrating Sample Magnetometry (VSM), and Scanning Electron Microscope (SEM).

The effects of pH, initial concentrations of Ni (II) and Cr (VI), adsorption kinetics, thermodynamics, and adsorption isotherm were studied.

#### Abbreviations

SEM, scanning electron microscope; TEM, transmission electron microscopy; VSM, vibrating sample magnetometry; XRD, powder X-Ray diffraction

#### Acknowledgements

This research was financially supported by Tehran University of Medical Sciences (TUMS), the Institute for Environmental Research (IER) (project No. 92-01-46-20998) which is highly appreciated. Thanks also go to Ms. A. Keivanshekouh at the Research Improvement Center of Shiraz University of Medical Sciences for improving the use of English in the manuscript.

#### Funding

This research was financially supported by Tehran University of Medical Sciences (TUMS), the Institute for Environmental Research (IER) (project No. 92-01-46-20998).

#### Availability of data and materials section

The authors do not wish to share their data. All the necessary data have been mentioned in the paper. If other researchers need our data for their studies, they can contact with first Autor via email.

#### Authors' contributions

MG supervised of this study, and participated in its design and coordination and helped to draft the manuscript. ANB participated in the design of the study, synthesized magnetic nanoadsorbent and prepared to draft the manuscript. AHM participated in the design of the study and in the sequence alignment. NR carried out to synthesize magnetic nanoadsorbent. MD performed the statistical analysis. All authors read and approved the final manuscript.

#### Competing interests

The authors declare that they have no competing interests.

#### Consent for publication

Not applicable.

#### Ethics approval and consent to participate

Not applicable.

#### Author details

[1]Center for Water Quality Research, Institute for Environmental Research (IER), Tehran University of Medical Sciences, Tehran, Iran. [2]Department of Environmental Health Engineering, School of Public Health Science, Tehran University of Medical Sciences, Tehran, Iran. [3]Center for Solid Waste Research, Institute for Environmental Research (IER), Tehran University of Medical Sciences, Tehran, Iran. [4]Research Center for Environmental Health Technology, Iran University of Medical Sciences, Tehran, Iran. [5]Environmental Health Department, School of Public Health, Iran University of Medical Sciences, Tehran, Iran. [6]Center for Air Pollution Research (CAPR), Institute for Environmental Research (IER), Tehran University of Medical Sciences, Tehran 1417613151, Iran. [7]Environmental Health Department, School of Public Health, Shiraz University of Medical Sciences, Shiraz, Iran.

Received: 27 December 2015 Accepted: 28 June 2016
Published online: 26 July 2016

#### References

1. Aguado J, Arsuaga JM, Arencibia A, Lindo M, Gascón V. Aqueous heavy metals removal by adsorption on amine-functionalized mesoporous silica. J Hazard Mater. 2009;163(1):213–21.
2. Pehlivan E, Altun T. Biosorption of chromium (VI) ion from aqueous solutions using walnut, hazelnut and almond shell. J Hazard Mater. 2008;155(1):378–84.
3. Kumar PA, Ray M, Chakraborty S. Hexavalent chromium removal from wastewater using aniline formaldehyde condensate coated silica gel. J Hazard Mater. 2007;143(1):24–32.
4. López-Téllez G, Barrera-Díaz CE, Balderas-Hernández P, Roa-Morales G, Bilyeu B. Removal of hexavalent chromium in aquatic solutions by iron nanoparticles embedded in orange peel pith. Chem Eng J. 2011;173(2):480–5.
5. Gode F, Pehlivan E. Removal of Cr (VI) from aqueous solution by two Lewatit-anion exchange resins. J Hazard Mater. 2005;119(1):175–82.
6. Panneerselvam P, Morad N, Tan KA. Magnetic nanoparticle (Fe 3 O 4) impregnated onto tea waste for the removal of nickel (II) from aqueous solution. J Hazard Mater. 2011;186(1):160–8.
7. Hua M, Zhang S, Pan B, Zhang W, Lv L, Zhang Q. Heavy metal removal from water/wastewater by nanosized metal oxides: a review. J Hazard Mater. 2012;211:317–31.
8. Miretzky P, Cirelli AF. Cr (VI) and Cr (III) removal from aqueous solution by raw and modified lignocellulosic materials: a review. J Hazard Mater. 2010;180(1):1–19.
9. Owlad M, Aroua MK, Daud WAW, Baroutian S. Removal of hexavalent chromium-contaminated water and wastewater: a review. Water Air Soil Pollut. 2009;200(1–4):59–77.

10. Asgari A, Vaezi F, Nasseri S, Dördelmann O, Mahvi A, Fard ED. Removal of hexavalent chromium from drinking water by granular ferric hydroxide. Iranian J Environ Health Sci Eng. 2008;5(4):277–82.
11. Bazrafshan E, Mahvi AH, Naseri S, Mesdaghinia AR. Performance evaluation of electrocoagulation process for removal of chromium (VI) from synthetic chromium solutions using iron and aluminum electrodes. Turk J Eng Environ Sci. 2008;32(2):59–66.
12. Dakiky M, Khamis M, Manassra A, Mer'eb M. Selective adsorption of chromium (VI) in industrial wastewater using low-cost abundantly available adsorbents. Adv Environ Res. 2002;6(4):533–40.
13. Li Y-H, Ding J, Luan Z, Di Z, Zhu Y, Xu C, et al. Competitive adsorption of Pb 2+, Cu 2+ and Cd 2+ ions from aqueous solutions by multiwalled carbon nanotubes. Carbon. 2003;41(14):2787–92.
14. Huang S-H, Chen D-H. Rapid removal of heavy metal cations and anions from aqueous solutions by an amino-functionalized magnetic nano-adsorbent. J Hazard Mater. 2009;163(1):174–9.
15. Rafati L, Mahvi A, Asgari A, Hosseini S. Removal of chromium (VI) from aqueous solutions using Lewatit FO36 nano ion exchange resin. Int J Environ Sci Technol. 2010;7(1):147–56.
16. Chang Y-C, Chang S-W, Chen D-H. Magnetic chitosan nanoparticles: Studies on chitosan binding and adsorption of Co (II) ions. React Funct Polym. 2006;66(3):335–41.
17. Hao Y-M, Man C, Hu Z-B. Effective removal of Cu (II) ions from aqueous solution by amino-functionalized magnetic nanoparticles. J Hazard Mater. 2010;184(1):392–9.
18. Tan Y, Chen M, Hao Y. High efficient removal of Pb (II) by amino-functionalized Fe 3 O 4 magnetic nano-particles. Chem Eng J. 2012;191:104–11.
19. Sayar O, Amini MM, Moghadamzadeh H, Sadeghi O, Khan SJ. Removal of heavy metals from industrial wastewaters using amine-functionalized nanoporous carbon as a novel sorbent. Microchim Acta. 2013;180(3–4):227–33.
20. Cui Y, Liu S, Hu Z-J, Liu X-H, Gao H-W. Solid-phase extraction of lead (II) ions using multiwalled carbon nanotubes grafted with tris (2-aminoethyl) amine. Microchim Acta. 2011;174(1–2):107–13.
21. Yuan P, Fan M, Yang D, He H, Liu D, Yuan A, et al. Montmorillonite-supported magnetite nanoparticles for the removal of hexavalent chromium [Cr (VI)] from aqueous solutions. J Hazard Mater. 2009;166(2):821–9.
22. Wang L, Bao J, Wang L, Zhang F, Li Y. One-Pot Synthesis and Bioapplication of Amine-Functionalized Magnetite Nanoparticles and Hollow Nanospheres. Chemistry-A Eur J. 2006;12(24):6341–7.
23. Zhou Y, Rahaman M. Hydrothermal synthesis and sintering of ultrafine CeO 2 powders. J Mater Res. 1993;8(07):1680–6.
24. Watson J, Cressey B, Roberts A, Ellwood D, Charnock J, Soper A. Structural and magnetic studies on heavy-metal-adsorbing iron sulphide nanoparticles produced by sulphate-reducing bacteria. J Magn Magn Mater. 2000;214(1):13–30.
25. Zhao Y-G, Shen H-Y, Pan S-D, Hu M-Q, Xia Q-H. Preparation and characterization of amino-functionalized nano-Fe3O4 magnetic polymer adsorbents for removal of chromium (VI) ions. J Mater Sci. 2010;45(19):5291–301.
26. Afkhami A, Saber-Tehrani M, Bagheri H. Simultaneous removal of heavy-metal ions in wastewater samples using nano-alumina modified with 2, 4-dinitrophenylhydrazine. J Hazard Mater. 2010;181(1):836–44.
27. Shen H, Pan S, Zhang Y, Huang X, Gong H. A new insight on the adsorption mechanism of amino-functionalized nano-Fe 3 O 4 magnetic polymers in Cu (II), Cr (VI) co-existing water system. Chem Eng J. 2012;183:180–91.
28. Guo X, Du B, Wei Q, Yang J, Hu L, Yan L, et al. Synthesis of amino functionalized magnetic graphenes composite material and its application to remove Cr (VI), Pb (II), Hg (II), Cd (II) and Ni (II) from contaminated water. J Hazard Mater. 2014;278:211–20.
29. Nassar NN. Kinetics, equilibrium and thermodynamic studies on the adsorptive removal of nickel, cadmium and cobalt from wastewater by superparamagnetic iron oxide nanoadsorbents. Can J Chem Eng. 2012;90(5):1231–8.
30. Mobasherpour I, Salahi E, Pazouki M. Removal of nickel (II) from aqueous solutions by using nano-crystalline calcium hydroxyapatite. J Saudi Chem Soc. 2011;15(2):105–12.
31. Abbott M, Smith J, Van Ness H. Introduction to chemical engineering thermodynamics: McGraw-Hill. 2001.
32. Freundlich H, Heller W. The adsorption of cis-and trans-azobenzene. J Am Chem Soc. 1939;61(8):2228–30.
33. Ho Y, Ng J, McKay G. Removal of lead (II) from effluents by sorption on peat using second-order kinetics. Sep Sci Technol. 2001;36(2):241–61.
34. Ho Y-S, McKay G. Pseudo-second order model for sorption processes. Process Biochem. 1999;34(5):451–65.
35. Javadian H, Taghavi M. Application of novel Polypyrrole/thiol-functionalized zeolite Beta/MCM-41 type mesoporous silica nanocomposite for adsorption of Hg 2+ from aqueous solution and industrial wastewater: Kinetic, isotherm and thermodynamic studies. Appl Surf Sci. 2014;289:487–94.
36. Qu R, Zhang Y, Sun C, Wang C, Ji C, Chen H, et al. Adsorption of Hg (II) from an aqueous solution by silica-gel supported diethylenetriamine prepared via different routes: kinetics, thermodynamics, and isotherms. J Chem Eng Data. 2009;55(4):1496–504.
37. Rostamian R, Najafi M, Rafati AA. Synthesis and characterization of thiol-functionalized silica nano hollow sphere as a novel adsorbent for removal of poisonous heavy metal ions from water: Kinetics, isotherms and error analysis. Chem Eng J. 2011;171(3):1004–11.
38. Yuh-Shan H. Citation review of Lagergren kinetic rate equation on adsorption reactions. Scientometrics. 2004;59(1):171–7.
39. Najafi M, Yousefi Y, Rafati A. Synthesis, characterization and adsorption studies of several heavy metal ions on amino-functionalized silica nano hollow sphere and silica gel. Sep Purif Technol. 2012;85:193–205.
40. Bhattacharya A, Naiya T, Mandal S, Das S. Adsorption, kinetics and equilibrium studies on removal of Cr (VI) from aqueous solutions using different low-cost adsorbents. Chem Eng J. 2008;137(3):529–41.
41. Mahdavi S, Jalali M, Afkhami A. Removal of heavy metals from aqueous solutions using Fe3O4, ZnO, and CuO nanoparticles. J Nanopart Res. 2012;14(8):1–18.
42. Gupta VK, Ali I. Removal of lead and chromium from wastewater using bagasse fly ash—a sugar industry waste. J Colloid Interface Sci. 2004;271(2):321–8.
43. Malkoc E, Nuhoglu Y. Investigations of nickel (II) removal from aqueous solutions using tea factory waste. J Hazard Mater. 2005;127(1):120–8.
44. Chen J, Hao Y, Chen M. Rapid and efficient removal of Ni2+ from aqueous solution by the one-pot synthesized EDTA-modified magnetic nanoparticles. Environ Sci Pollut Res. 2014;21(3):1671–9.
45. Chen R, Chai L, Li Q, Shi Y, Wang Y, Mohammad A. Preparation and characterization of magnetic Fe3O4/CNT nanoparticles by RPO method to enhance the efficient removal of Cr (VI). Environ Sci Pollut Res. 2013;20(10):7175–85.
46. Malay DK, Salim AJ. Comparative study of batch adsorption of fluoride using commercial and natural adsorbent. Res J Chem Sci ISSN. 2011;2231:606X.
47. Yuan P, Liu D, Fan M, Yang D, Zhu R, Ge F, et al. Removal of hexavalent chromium [Cr (VI)] from aqueous solutions by the diatomite-supported/unsupported magnetite nanoparticles. J Hazard Mater. 2010;173(1):614–21.
48. Rao M, Parwate A, Bhole A. Removal of Cr 6+ and Ni 2+ from aqueous solution using bagasse and fly ash. Waste Manag. 2002;22(7):821–30.
49. Heidari A, Younesi H, Mehraban Z. Removal of Ni (II), Cd (II), and Pb (II) from a ternary aqueous solution by amino functionalized mesoporous and nano mesoporous silica. Chem Eng J. 2009;153(1):70–9.